

Can sodium 1-alkylsulfonates participate in the sodium dodecyl sulfate micelle formation?

Ola Grabowska¹, Krzysztof Żamojć^{1*}, Michał Olewniczak², Lech Chmurzyński¹,
and Dariusz Wyrzykowski¹

¹ Faculty of Chemistry, University of Gdansk, Wita Stwosza 63, 80-308 Gdansk, Poland

² Faculty of Chemistry, Gdansk University of Technology, Narutowicza 11/12, 80-233 Gdansk, Poland

* Corresponding author: krzysztof.zamojcz@ug.edu.pl, +48 58 523 50 57 (K.Ż.)

Abstract

The aggregation behavior of sodium dodecyl sulfate (SDS) was studied in an aqueous solution in the presence of increasing concentrations of selected sodium 1-alkylsulfonates, namely sodium 1-octanesulfonate, sodium 1-decanesulfonate, and sodium 1-dodecanesulfonate. The critical micelle concentration (CMC) of SDS was determined by conductivity and fluorescence intensity measurements. The steady-state fluorescence quenching experiments with pyrene as a fluorescent probe were performed to obtain micellar aggregation numbers (N_{agg}) of the surfactant. The thermodynamic parameters of micellization (ΔG_{mic}^0 for all studied systems; ΔH_{mic}^0 and ΔS_{mic}^0 for sodium 1-dodecanesulfonate) have been determined and compared. The influence of alkyl chain length and concentration of the selected sodium 1-alkylsulfonates on the values of CMC, N_{agg} , ΔG_{mic}^0 , ΔH_{mic}^0 , and ΔS_{mic}^0 of SDS has been discussed. As it was found, all selected for the experiments electrolytes decrease significantly the CMC of the surfactant, while an opposite effect is observed for N_{agg} values. The obtained experimental results have been supported by theoretical calculations. Interestingly, it has been proven that solely the molecules of sodium 1-dodecanesulfonate (of the same carbon chain length) may act as the SDS mimetics – they are not recognized by SDS as the ones with a different structure and consequently are allowed to participate in the formation of the surfactant's micelles.

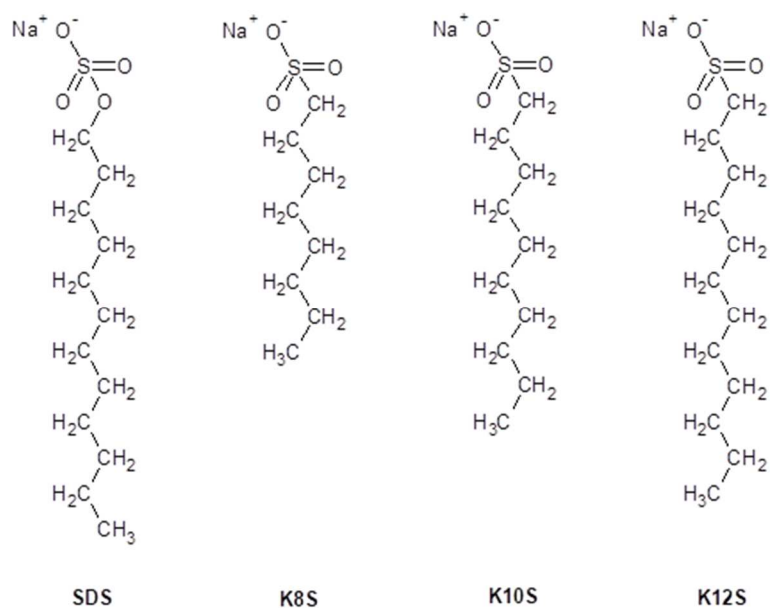
Keywords: sodium dodecyl sulfate; sodium 1-alkylsulfonates; critical micelle concentration; micellar aggregation number; thermodynamic parameters; fluorescence spectroscopy; conductivity; molecular dynamics.

1. Introduction

Surfactants, considering their structure and charge of the hydrophilic parts of the molecule, can be divided into cationic, anionic, amphoteric and nonionic ones [1]. The surface properties of these amphiphilic molecules, such as lipophilicity, viscosity, solubilization capacity, adsorption at the interface, self-assembly or micelle formation [2], are induced by the hydrophobic interaction between hydrocarbon parts of the surfactant molecules balanced by their hydration and electrostatic

38 repulsive effects [3] and play an important role in many natural and industrial
39 applications, *i.e.* detergent and pharmaceutical industries, food technology, and
40 petroleum recovery processes [4]. The tendency of surfactants to self-aggregate is
41 with no doubt one of the most fascinating aspects of these particles, while micelles
42 remain one of the central topics of study within surface and colloid chemistry [5].
43 Important experimental characteristics describing micelles are the critical micelle
44 concentration (CMC; the concentration where they are formed) [6], kinetic features
45 (such as the micellar lifetime and reaction rates) [7], their size, shape, dispersity in
46 a solution [8], aggregation numbers (N_{agg} ; the amount of surfactant molecules making
47 up a micelle) [9] as well as the thermodynamics [10] of the micellization process
48 (entropy is believed to be the major driving force for micellization in aqueous
49 solutions). All these parameters are sensitive to numerous internal (*e.g.*, hydrophobic
50 structure and head group type [11]) and external (surfactant concentration [12],
51 pressure [13], pH [14], temperature [15], ionic strength [16], solvent properties [17],
52 presence of electrolyte [18] and non-electrolyte [19] additives, applied technique [20],
53 *etc.*) factors and impact even on biological properties (it has been proven for example
54 that the highest antimicrobial properties are observed at concentrations below CMC
55 [21]). Therefore, it is of great importance from the practical point of view –
56 particularly when the real systems are investigated – to consider the influence of
57 additives and other factors on the features of surfactants [22].

58 Generally, added electrolytes are known to affect the aggregation behavior of the
59 ionic surfactants, which is attributed entirely to the counter-ion effect [23]. However,
60 there are reports indicating that a co-ion, depending upon its and surfactant's
61 structures, can also affect the micellization phenomenon [24]. In this paper, we report
62 the aggregation behavior of sodium dodecyl sulfate (SDS) in the presence of selected
63 sodium 1-alkylsulfonates of different chain lengths, namely sodium
64 1-octanesulfonate (K8S), sodium 1-decanesulfonate (K10S), and sodium
65 1-dodecanesulfonate (K12S) studied by steady-state fluorescence spectroscopy and
66 conductivity measurements and supported by molecular dynamics simulations. All
67 chosen sodium 1-alkylsulfonates are structurally very similar to the SDS surfactant
68 (**Figure 1**). In sodium dodecyl sulfate the sulfur of a headgroup is linked to the
69 carbon atom via an oxygen atom, while in sulfonates it is linked directly to a carbon
70 chain of an appropriate length (8, 10, and 12 carbon atoms in the case of K8S, K10S,
71 and K12S, respectively). According to our knowledge, the determination of critical
72 micelle concentrations (CMC), micellar aggregation numbers (N_{agg}) and
73 thermodynamic parameters of micellization of SDS in the presence of the chosen
74 sulfonates has been never performed, although such a need has been signaled
75 previously [25]. Can molecules with a structure similar to SDS act as the surfactant's
76 mimetics and be incorporated into its micelles? Or maybe SDS molecules recognize
77 that other molecules have a slightly different structure and consequently do not
78 allow them to participate in the formation of the surfactant's micelles? The search for
79 the answers to questions raised has prompted us to embark on these studies.



80

81 **Figure 1.** Chemical structures of SDS, K8S, K10S, and K12S.

82 2. Experimental

83 2.1. Materials

84 Sodium dodecyl sulfate (SDS, $\geq 99.0\%$), sodium 1-octanesulfonate (K8S, $\geq 99\%$),
 85 sodium 1-decanesulfonate (K10S, $\geq 99\%$), sodium 1-dodecanesulfonate (K12S, $\geq 99\%$),
 86 pyrene ($\geq 97\%$), cetylpyridinium chloride (CPC, $\geq 98\%$), and sodium chloride ($\geq 99\%$)
 87 were acquired from Merck (Poland) and used without additional purification as
 88 received. For all solutions preparation, double-distilled water with a conductivity of
 89 less than $0.18 \mu\text{S cm}^{-1}$ was employed. The studies of the aggregation behavior of SDS
 90 were performed in aqueous solutions of K8S, K10S, K12S, and NaCl used at low
 91 concentrations (1-8 mM), because it is difficult to get reliable conductivity results in
 92 the high ionic strength [25,26]. Due to the limited solubility of K12S in water its
 93 highest concentration was set at 4 mM.

94 2.2. Methods

95 2.2.1. Steady-state fluorescence spectroscopy

96 The Cary Eclipse Varian (Agilent, Santa Clara, CA, USA) spectrofluorometer,
 97 equipped with a temperature controller and a 1.0 cm multicell holder, was used to
 98 measure the fluorescence intensities. All experiments were conducted at 298.15 K.

99 The fluorescence emission spectra of pyrene ($c = 2 \mu\text{M}$; $V = 2 \text{ mL}$; $\lambda_{\text{ex}} = 340 \text{ nm}$; the
 100 excitation and emission slit widths set at 5 nm) dissolved in: (i) 1, 2, 4, and 8 mM K8S;
 101 (ii) 1, 2, 4, and 8 mM K10S; (iii) 1, 2, and 4 mM K12S; (iv) water, 1, 2, 4, and 8 mM
 102 NaCl were recorded from 360 to 500 nm in both the absence and presence of
 103 increasing amounts of SDS in order to determine the CMC values (up to 11 mM). The

104 values obtained are the means of two separate experiments. All spectra were
105 recorded in triplicate for each experiment.

106 In order to determine the N_{agg} values the fluorescence intensity of pyrene ($c = 2 \mu\text{M}$;
107 $V = 2 \text{ mL}$; $\lambda_{ex} = 340 \text{ nm}$; $\lambda_{em} = 375 \text{ nm}$; the excitation and emission slit widths set at 5
108 nm) dissolved in a mixture of 10 mM SDS and: (i) 1, 2, 4, and 8 mM K8S; (ii) 1, 2, 4,
109 and 8 mM K10S; (iii) 1, 2, and 4 mM K12S; (iv) water, 1, 2, 4, and 8 mM NaCl was
110 measured in the absence and presence of increasing concentrations of the quencher,
111 cetylpyridinium chloride, CPC (up to 19.5 μM). The same titration was performed
112 four times, thus all obtained values are means from four separate experiments.

113 **2.2.2. Conductivity measurements**

114 Conductometric measurements for all studied systems were performed at 298.15 K
115 using a microtitration unit (Cerko Lab System, Poland) fitted with a 5 mL syringe
116 (Hamilton, Poland) and a CD-201 conductometric cell (Hydromet, Poland). The
117 details of the measuring devices and experimental setup have been described
118 previously [27]. The experiment consisted of injecting 0.01 mL of the titrant solution
119 comprising SDS ($c = 60 \text{ mM}$) and the appropriate ligand of different concentrations
120 (1, 2, 4, and 8 mM K8S; 1, 2, 4, and 8 mM K10S; 1, 2, and 4 mM K12S; water, 1, 2, 4,
121 and 8 mM NaCl), into the reaction cell containing the ligand solution only. In the case
122 of 1, 2, and 4 mM K12S the conductometric titrations were additionally performed at
123 308.15 K and 318.15 K.

124 **2.2.3. Molecular Dynamics (MD) simulation protocol**

125 All simulated systems were built using CHARMM-GUI server [28] and were
126 performed using Gromacs 2020 [29] with Plumed 2.6 plugin [30] and applying
127 CHARMM36m force field [31]. TIP3P model was used for water molecules. The
128 simulations were carried out in the isothermal-isobaric (NPT) ensemble using
129 periodic boundary conditions. Nose-Hoover algorithm [32] with a coupling constant
130 of 1 ps was used to keep the temperature at 300.15 K, while the Parrinello-Rahman
131 algorithm [33] with a coupling time of 5 ps was used to maintain the pressure of
132 1 bar. Electrostatic interactions were calculated with the Particle Mesh Ewald method
133 [34] using a cut-off radius equal to 1.2 nm (with the switching function applied from
134 the distance of 1 nm) and the Fourier grid spacing of 0.12 nm. Van der Waals
135 interactions were calculated with Lennard-Jones potential with a cut-off radius of
136 1 nm. The Hydrogen Mass Repartitioning approach [35] was used, which enabled us
137 to use the 4 fs time step of integration of the equations of motion. Minimization and
138 equilibration of the systems were performed following the default CHARMM-GUI
139 Membrane Builder protocol [36].

140 The initial micelle system was composed of 70 dodecyl sulfate anions placed in an
141 8.1x8.1x8.1 nm rectangular box filled with 16998 water molecules and 116 Na^+ and 46

142 Cl⁻ ions to provide 0.15 M ionic strength. Systems with mixed micelle compositions
143 were prepared by exchanging the proper amount of dodecyl sulfate anions (7, 21 or
144 35) to 1-alkylsulfonate anions; for each system, 2.5 μs-long trajectories were obtained.

145 2.2.4. Free energy calculations

146 The free energy profiles for the sulfonates association to SDS micelle were
147 determined with replica-exchange umbrella sampling method [37], using center-of-
148 mass distance between SDS micelle and sodium sulfonate as the reaction coordinate.
149 The initial configurations for US simulations were obtained with 100 ns-long steered-
150 MD simulations, in which one SDS molecule was replaced by sodium sulfonate
151 molecule and was pulled away from the SDS micelle with the harmonic constant of
152 500 kJ mol⁻¹ nm⁻².

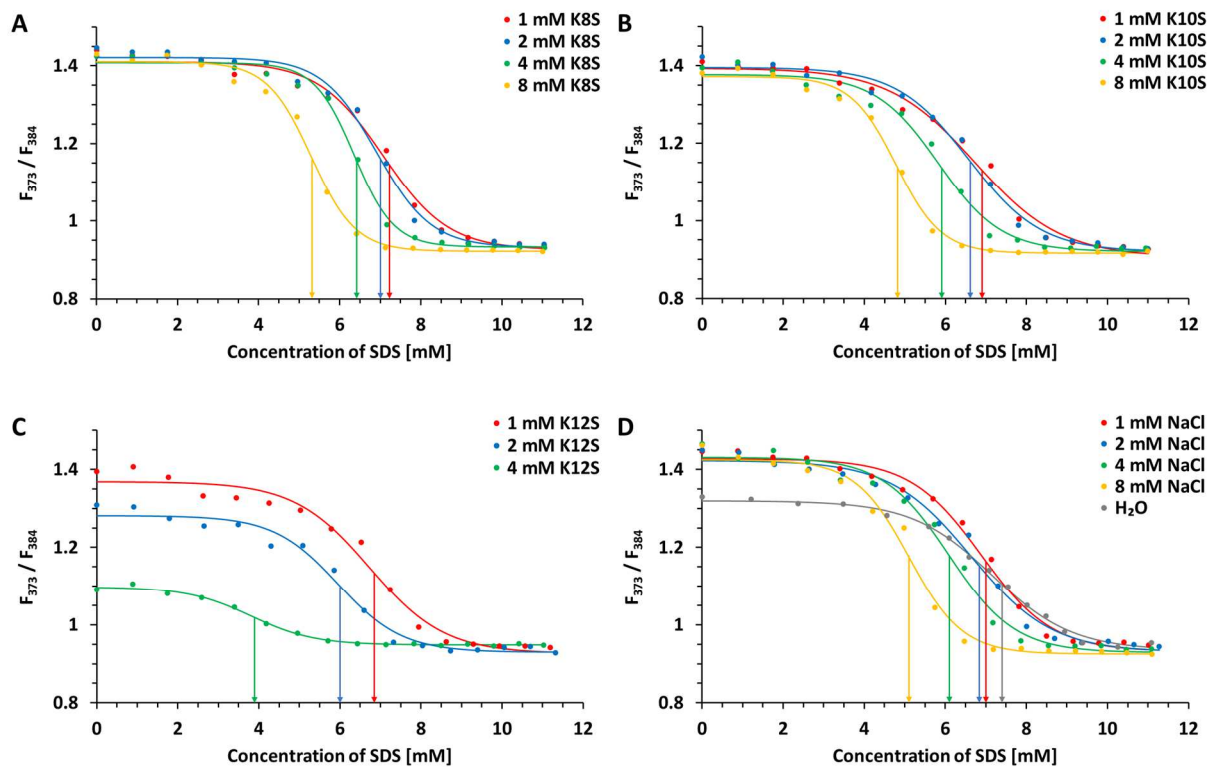
153 9 equally spaced US windows were used, spanning a 1-5.0 nm range of the reaction
154 coordinate. The spring constant of the harmonic biasing potential was set to 75 kJ
155 mol⁻¹ nm⁻² in each US window. Each of the US windows were simulated for 1.5 μs
156 and free energy profiles were determined using the weighted histogram analysis
157 method [38]. The same procedure was used to calculate the referential free energy
158 profile for SDS association to the micelle. Uncertainties were estimated using
159 bootstrap error analysis taking into account the correlation in the analyzed time
160 series.

161 3. Results and discussion

162 3.1. Critical micelle concentration

163 The CMC values of SDS in the presence of various concentrations of K8S, K10S, and
164 K12S (and NaCl as a reference) were obtained – among others – from steady-state
165 fluorescence spectroscopy measurements using pyrene, a well-known fluorescent
166 probe utilized for the micropolarity studies of its solubilization site in the micellar
167 interior [39]. When pyrene is excited at approximately 335-340 nm, its fluorescence
168 emission spectrum exhibits five typical vibronic peaks. The intensity ratio $\frac{F_{373}}{F_{384}}$ of the
169 first (solvent-sensitive band at 373 nm) and the third (solvent-insensitive band at 384
170 nm) vibronic peaks [40] is very sensitive to solvent polarity and therefore has been
171 widely used to measure the polarity of the microenvironment of the polycyclic
172 aromatic hydrocarbon (high values indicate polar environment) and CMC of
173 surfactants [41]. Thus, the ratio $\frac{F_{373}}{F_{384}}$ for pyrene was determined in the absence and
174 presence of increasing amounts of SDS (at various concentrations of K8S, K10S, K12S,
175 and NaCl). For all studied systems it decreased significantly with the increase of SDS
176 concentration (**Figure 2**). The inflection points of these curves indicate the CMC
177 values of the micellization of SDS, which are presented in **Table 1**.



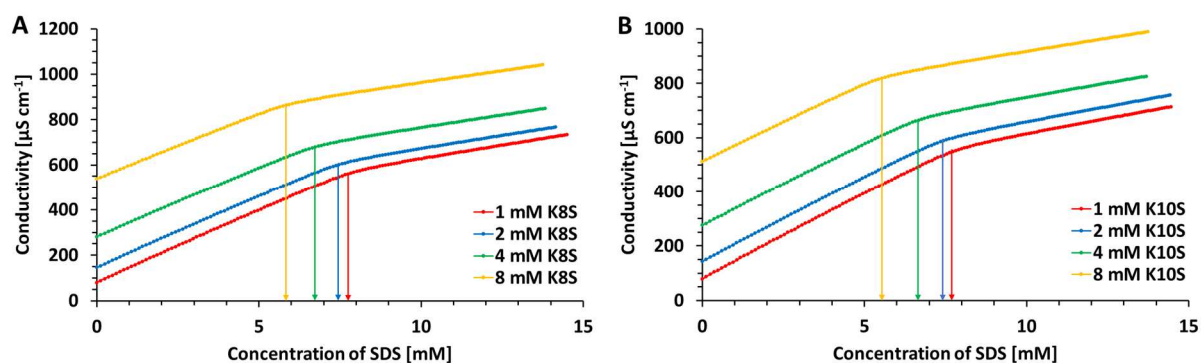


178

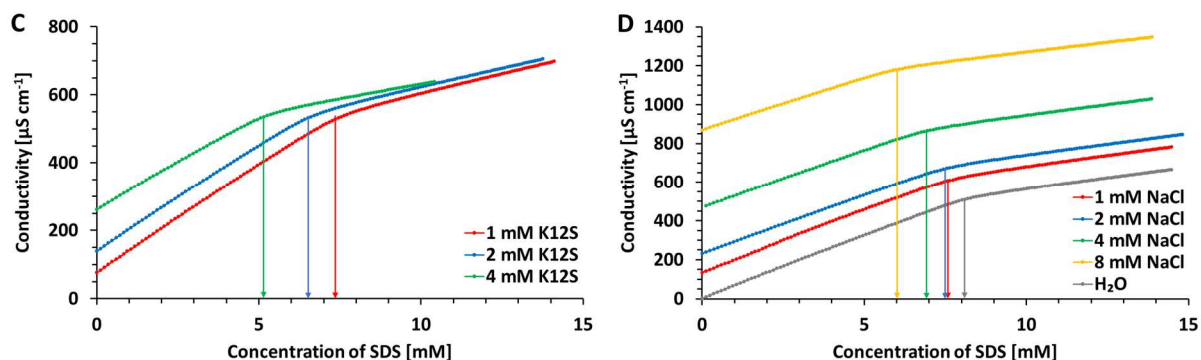
179

180 **Figure 2.** Plots of fluorescence intensity ratio $\frac{F_{373}}{F_{384}}$ for pyrene as a function of SDS
 181 concentration in the presence of various concentrations of K8S (A), K10S (B), K12S
 182 (C), and NaCl (D); $\lambda_{\text{ex}} = 340 \text{ nm}$; $c_{\text{pyrene}} = 2 \mu\text{M}$; 298.15 K.

183 Furthermore, the CMC values of SDS were obtained for all studied systems from
 184 conductivity measurements. The plots of conductivity (κ) *vs* the concentration of SDS
 185 determined in the presence of different concentrations of K8S, K10S, K12S, and NaCl
 186 are shown in **Figure 3**. It is known that the specific conductivity is linearly correlated
 187 to the surfactant concentration in both the premicellar and postmicellar regions, with
 188 the slope in the premicellar region greater than that in the postmicellar region [3],
 189 which is due to lower mobility of micelles when compared to monomers [26].
 190 Indeed, the plots exhibit two straight lines (both increasing with the increase of the
 191 concentration of SDS in the solution) intersecting at the point indicating the
 192 formation of the micelle. The CMC values are gathered in **Table 1**.



193



194

195 **Figure 3.** Plots of conductivity (κ) as a function of SDS concentration in the presence
 196 of various amounts of K8S (A), K10S (B), K12S (C), and NaCl (D); 298.15 K.

197 The value of CMC of SDS in water (in the absence of any added electrolyte) is in
 198 a great agreement with the previous reports [25,42]. From the inspection of **Figure 2**,
 199 **Figure 3**, and **Table 1** it can be clearly noticed that the CMC of SDS decreases very
 200 significantly with the increase of the concentration of the studied sodium
 201 1-alkylsulfonates and sodium chloride. The lower values of CMC of SDS in the
 202 presence of K8S, K10S, K12S, and NaCl suggest its stronger tendency to self-assemble
 203 (SDS solutions containing sulfonates are more associated [43]) and form micelles
 204 under these conditions (micellization is favored in the occurrence of all studied salts
 205 in comparison to pure surfactant) [26,44]. In the case of sodium chloride the
 206 significant reduction of CMC values is related to the presence of additional ions from
 207 salt dissociation and their interactions with the SDS hydrophilic parts, monomers
 208 which are in the equilibrium with micelles or interactions with water molecules from
 209 the aqueous pseudophase [22,45]. The interactions of sodium cations with the
 210 negatively charged head of SDS micelles result in the reduction of electrostatic
 211 repulsions thereby increasing micelle stability and consequently, lowering the critical
 212 micelle concentration [22]. Such a trend has been observed previously for SDS/NaCl
 213 and SDS/KCl systems [22,25,46,47]. Furthermore, a comparison of CMC values of
 214 SDS determined in the presence of homologous series of the studied sodium
 215 sulfonates demonstrates that increasing the length of their hydrocarbon chain has the
 216 tendency of lowering the concentration of surfactant at which aggregation is
 217 initiated. However, NaCl exhibits very similar to K8S and K10S effect on the
 218 lowering the CMC of SDS – the values of critical micelle concentration in these two
 219 sulfonates are comparable and the co-ions seem not to have any other effect on the
 220 CMC of SDS than chloride ion. It means that the organic anions of K8S and K10S do
 221 not participate in the stabilization of micelles. It is in great accordance with previous
 222 reports concluding that there is indeed no co-ion effect on the micellization
 223 parameters of anionic surfactants by acetate, propionate and butyrate ions [25,48].
 224 Interestingly, this is not the case for K12S – all studied solutions of that sodium 1-
 225 alkylsulfonate reduce CMC much stronger than K8S, K10S, and NaCl at the same
 226 concentrations. Specifically, 2 mM K12S decreases the CMC similarly to K8S, K10S,
 227 and NaCl, but at concentrations twice higher, while 4 mM K12S exhibits significantly

228 greater impact when compared to 8 mM K8S, 8 mM K10S, and 8 mM NaCl. Hence, it
 229 can be supposed that K12S participates in the formation of the SDS micelles on
 230 account of identical to SDS hydrophobic chain length.

231 **Table 1.** Critical micelle concentration (CMC) obtained by both, conductometric
 232 titration (^C) and steady-state fluorescence spectroscopy (^F), degree of counter-ion
 233 binding (β), standard Gibb's free energy change (ΔG_{mic}^0) and aggregation number
 234 (N_{agg}) values of the micellization of SDS in the presence of various concentrations of
 235 K8S, K10S, K12S, and NaCl.

| System | CMC [mM] | β | ΔG_{mic}^0 [kJ mol ⁻¹] | N_{agg} | System | CMC [mM] | β | ΔG_{mic}^0 [kJ mol ⁻¹] | N_{agg} |
|-----------|--------------------------------------|---------|--|-----------|-----------|--------------------------------------|---------|--|-----------|
| 1 mM K8S | 7.8 ^C 7.2 ^F | 0.622 | -35.65 | 59 | 1 mM K12S | 7.3 ^C 6.8 ^F | 0.631 | -36.12 | 66 |
| 2 mM K8S | 7.4 ^C 7.0 ^F | 0.626 | -35.95 | 62 | 2 mM K12S | 6.5 ^C 6.0 ^F | 0.642 | -36.83 | 68 |
| 4 mM K8S | 6.7 ^C 6.4 ^F | 0.626 | -36.35 | 67 | 4 mM K12S | 5.1 ^C 3.9 ^F | 0.674 | -38.55 | 76 |
| 8 mM K8S | 5.8 ^C 5.3 ^F | 0.628 | -36.98 | 69 | Water | 8.1 ^C 7.4 ^F | 0.643 | -35.96 | 58 |
| 1 mM K10S | 7.7 ^C 6.9 ^F | 0.630 | -35.88 | 64 | 1 mM NaCl | 7.6 ^C 7.0 ^F | 0.630 | -35.93 | 60 |
| 2 mM K10S | 7.3 ^C 6.6 ^F | 0.631 | -36.12 | 67 | 2 mM NaCl | 7.5 ^C 6.8 ^F | 0.622 | -35.81 | 65 |
| 4 mM K10S | 6.6 ^C 5.9 ^F | 0.640 | -36.72 | 68 | 4 mM NaCl | 6.9 ^C 6.1 ^F | 0.621 | -36.12 | 68 |
| 8 mM K10S | 5.5 ^C 4.8 ^F | 0.657 | -37.85 | 72 | 8 mM NaCl | 6.0 ^C 5.1 ^F | 0.622 | -36.70 | 70 |

236

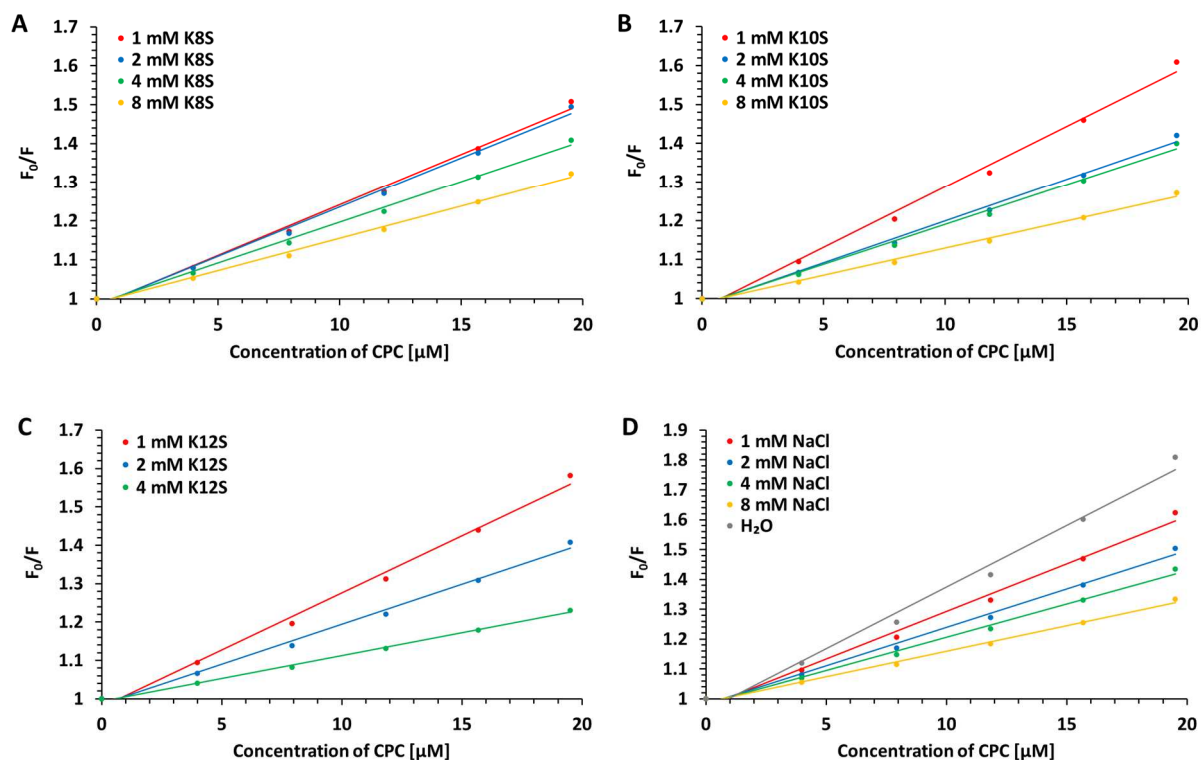
237 3.2. Thermodynamics of micelle formation

238 The micellization behavior of surfactants can be influenced by
 239 structural/environmental modification which can be assessed by evaluating
 240 numerous thermodynamic parameters [26]. The standard Gibb's free energy change
 241 of micellization (ΔG_{mic}^0) per mole of monomer of SDS was calculated for all the
 242 studied systems from conductivity measurements using the following equation:
 243 $\Delta G_{mic}^0 = (1 + \beta)RT \ln X_{CMC}$, where X_{CMC} denotes CMC in mole fraction unit, R is the
 244 gas constant, T is the absolute temperature, and $\beta (= 1 - \alpha)$ is a degree of counter-ion
 245 binding (the values of the micelle ionization degree α were calculated as the ratio of
 246 the slopes of the two linear fragments of conductivity-concentration plot above and
 247 below CMC) [49]. The appropriate values of ΔG_{mic}^0 are listed in **Table 1**. It can be
 248 clearly observed that with increasing the alkyl chain length and concentration of the
 249 added sodium 1-alkylsulfonate the micellization process becomes more favorable
 250 (ΔG_{mic}^0 decreases). An opposite effect is observed for β – its values increase very
 251 slightly (the electrolyte anions are known to cause a much smaller change in the

252 values of β for SDS than the cations [50]) with increasing the concentration and
253 length of the sulfonates, which means that the binding of the counter-ions to the
254 micelles increases [25]. The additional studies conducted at various temperatures for
255 1, 2, and 4 mM K12S (**Figure S1** in Electronic Supplementary Information) enabled
256 determination of the values of the standard enthalpy (ΔH_{mic}^0) and then the standard
257 entropy (ΔS_{mic}^0) changes of micellization per mole of surfactant according to the
258 following equations: $\Delta H_{\text{mic}}^0 = -(1 + \beta)RT^2 \frac{d \ln X_{\text{CMC}}}{dT}$ (where $\frac{d \ln X_{\text{CMC}}}{dT}$ corresponds to the
259 slopes of the plots in Figure S1) and $\Delta S_{\text{mic}}^0 = \frac{\Delta H_{\text{mic}}^0 - \Delta G_{\text{mic}}^0}{T}$ [49]. The standard enthalpy
260 changes of micellization of SDS in 1, 2, and 4 mM K12S are -6.74 , -6.24 , and -4.68 kJ
261 mol^{-1} , respectively. ΔH_{mic}^0 are rather small and negative indicating that micellization
262 process is exothermic. The standard entropy changes of micellization of SDS are 99,
263 103, and 114 $\text{J mol}^{-1} \text{K}^{-1}$ in 1, 2, and 4 mM K12S, respectively. ΔS_{mic}^0 is positive and
264 increases with the increase of K12S concentration. The large entropy change values
265 support the spontaneous micellization and hint that process is driven by an increase
266 in entropy [42].

267 3.3. Aggregation number of SDS micelles

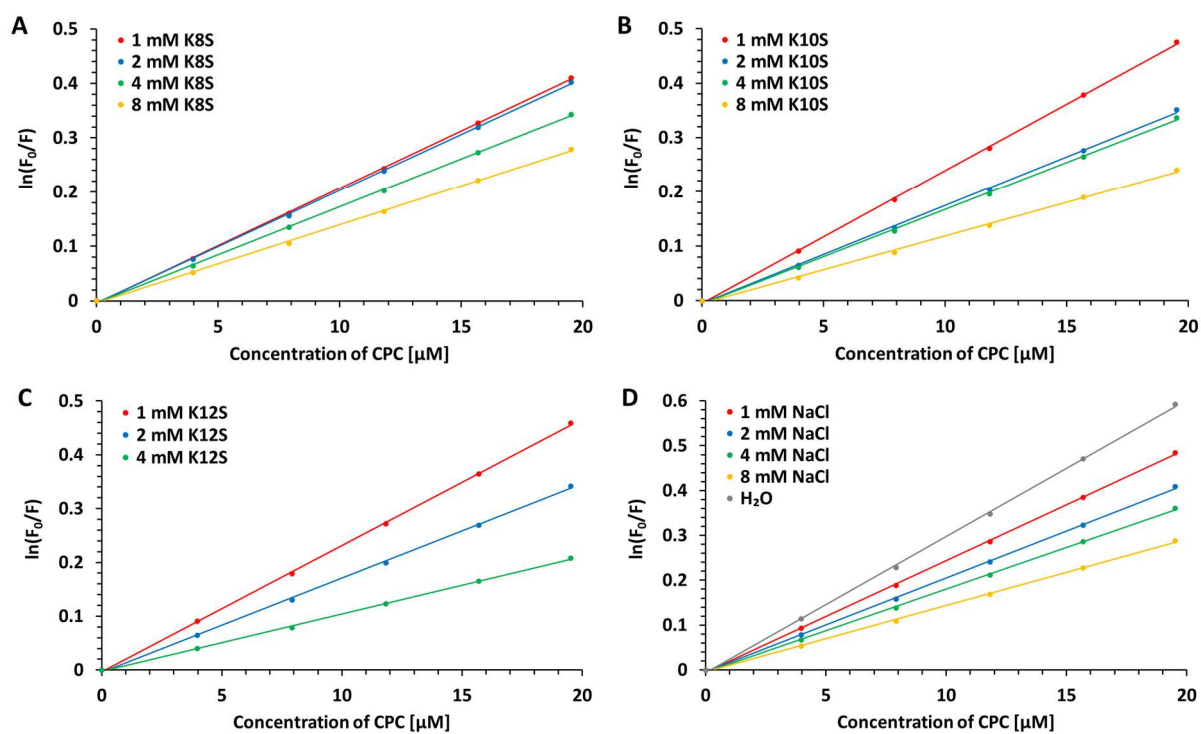
268 The mean aggregation numbers of SDS micelles were determined by fluorescence
269 quenching method using pyrene as fluorescent probe and cetylpyridinium chloride
270 as quencher molecule. The most important advantage of this method is that the
271 aggregation number can be determined also when the micelles interact in solution
272 [51]. N_{agg} values of SDS in the presence of various concentrations of K8S, K10S, K12S,
273 and NaCl were calculated from the slopes of the plots of $\ln\left(\frac{F_0}{F}\right)$ versus $[Q]$ according
274 to the equation: $\ln\left(\frac{F_0}{F}\right) = \frac{N_{\text{agg}}[Q]}{c - \text{CMC}}$, where F_0 and F are the fluorescence intensities in the
275 absence and presence of quencher, respectively, c is the total surfactant concentration
276 (higher than CMC; here 10 mM), and $[Q]$ is quencher (CPC) concentration [52]. The
277 highest CPC concentration ($\sim 20 \mu\text{M}$) was much below its CMC ($\sim 100 \mu\text{M}$), while the
278 concentration of pyrene ($2 \mu\text{M}$) was much lower than the micelle concentration, what
279 ensures quenching of the fluorescence of pyrene molecules that are solubilized in the
280 micelles. This is indicated by the high values of the Stern–Volmer constants (K_{SV} from
281 11860 M^{-1} to 41300 M^{-1}) obtained from the strictly linear (R^2 from 0.988 to 0.997) plots
282 of Stern–Volmer equation, $\frac{F_0}{F} = 1 + K_{\text{SV}}[Q]$ (**Figure 4**). The plots of $\ln\left(\frac{F_0}{F}\right)$ vs the
283 concentration of CPC for 10 mM SDS are shown in **Figure 5**. The N_{agg} values as
284 obtained from the slopes of the straight lines are listed in **Table 1**. It can be observed
285 that aggregation number of SDS increases in the presence of studied sodium
286 1-alkylsulfonates and sodium chloride, as is always observed for ionic surfactants
287 [41]. Furthermore, the higher the length of the hydrocarbon chain of the present in
288 the system sulfonates salts, the higher the average micellar aggregation number. This
289 is an expected behavior because, in general, the value of the micelle aggregation
290 number increases as the CMC value decreases [41,42].



291

292

293 **Figure 4.** Stern-Volmer plots for the quenching of pyrene as a function of CPC
 294 concentration (for 10 mM SDS; in the presence of various concentrations of K8S,
 295 K10S, K12S, and NaCl); $\lambda_{\text{ex}} = 340 \text{ nm}$; $\lambda_{\text{em}} = 375 \text{ nm}$; $c_{\text{pyrene}} = 2 \mu\text{M}$; 298.15 K.



296

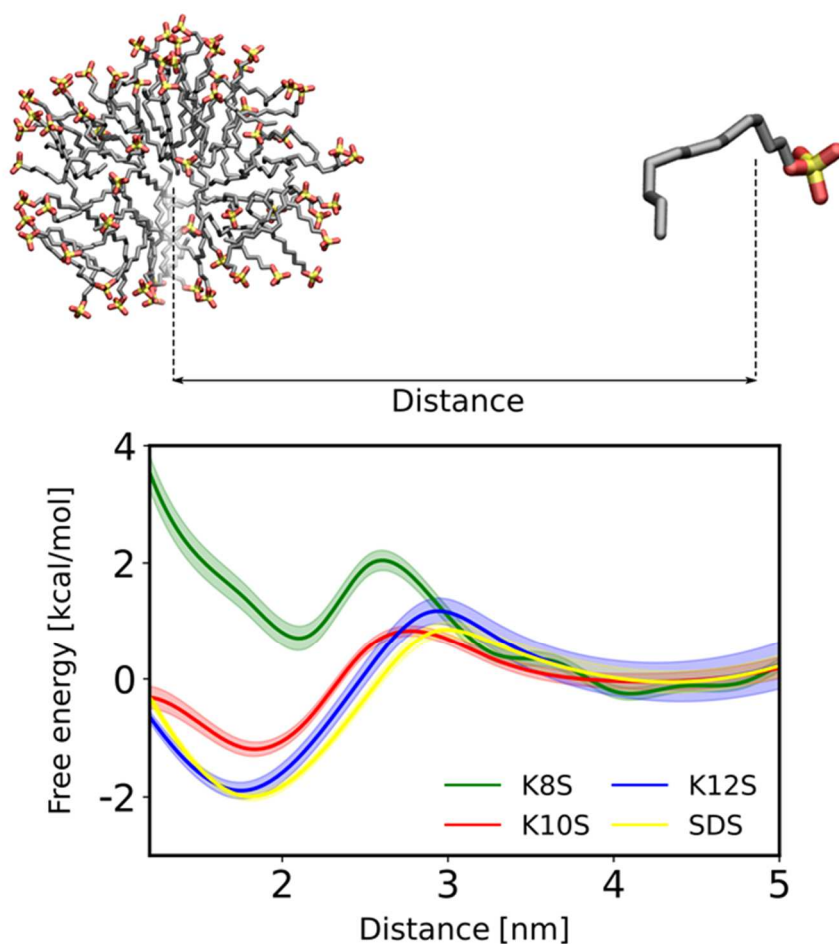
297

298 **Figure 5.** Plots of $\ln \frac{F_0}{F}$ of pyrene as a function of CPC concentration (for 10 mM SDS;
 299 in the presence of various concentrations of K8S, K10S, K12S, and NaCl); $\lambda_{\text{ex}} = 340$
 300 nm ; $\lambda_{\text{em}} = 375 \text{ nm}$; $c_{\text{pyrene}} = 2 \mu\text{M}$; 298.15 K.

301

3.4. Free energy of sulfonates association to SDS micelles

302 To investigate the possibility of sodium 1-alkylsulfonates participation in the SDS
 303 micelle formation, we firstly used umbrella sampling method to calculate the free
 304 energy profiles for sulfonates association to the SDS micelle. As can be seen on
 305 **Figure 6**, our results clearly illustrate that elongating of the alkyl chain results in
 306 growing affinity of the sulfonate to the SDS micelle. Furthermore, the free energy
 307 profile for K12S matches exactly the referential profile for the SDS association to the
 308 micelle. As affinities to the micelle for K8S and K10S are lower than affinity for SDS
 309 self-association to the micelle, one can expect that in the presence of either K8S or
 310 K10S and SDS in solution, formed micelle will be composed of only SDS molecules.
 311 In the case of K12S however, the resemblance of the affinities for K12S to the micelle
 312 and SDS self-association hints that K12S molecules can form micelles along with the
 313 SDS molecules, which may explain the significant reduction of CMC observed in the
 314 experiments.



315

316 **Figure 6.** (Top) Structural representation of the reaction coordinate used in the study.
 317 The image was created using VMD [53]. (Bottom) Free energy profiles for the
 318 sulfonates association to the SDS micelle.

319

320

3.5. Stability of the mixed-composition micelles

321 In order to explore the stability of the mixed-composition micelles, we prepared
 322 systems with 10, 30 or 50% of dodecyl sulfate anions replaced by 1-alkylsulfonate
 323 anions, which were then simulated for 2.5 μ s. During the simulations, the SDS core of
 324 the micelles remained intact, however, we observed events of sulfonates dissociation
 325 from the micelle to the solvent. To compare this effect between simulated systems,
 326 we calculated the actual composition of micelles from the last microsecond of
 327 simulation (Table 2). The sulfonate molecules were treated as the part of micelle
 328 when their distance to the centre-of-mass of SDS molecules were smaller than 2.7 nm.

329 **Table 2.** Average composition of the micelles during the last 1 μ s of simulations.

| Initial composition of micelle (fraction of sulfonates [%]) | Average fraction of sulfonates in the micelles [%] | | |
|---|--|--------------------|-------------------|
| | K8S | K10S | K12S |
| 10 | 8,1 (\pm 2,4) | 3,7 (\pm 2,8) | 8,7 (\pm 1,7) |
| 30 | 17,3 (\pm 6,1) | 19,4 (\pm 4,5) | 21,0 (\pm 3,6) |
| 50 | 28,1 (\pm 10,2) | 22,7 (\pm 12,1) | 34,4 (\pm 8,1) |

330 As, according to the calculated free energy profiles, K8S and K10S molecules are less
 331 preferred to participate in the micelle formation than SDS, the K8S/SDS and
 332 K10S/SDS micelles can be treated as the referential states, stabilized mostly by the
 333 fact that the resultant number of SDS molecules in the systems is below their
 334 aggregation number. Although highly dynamic nature of the sulfonates exchange
 335 between the solvent and micelle, on average more K12S molecules participate in the
 336 micelle formation, in contrast to shorter sulfonates, what is particularly visible in the
 337 initial 50:50 investigated systems.

338 4. Conclusions

339 The aggregation behavior of sodium dodecyl sulfate (SDS) surfactant was studied in
 340 aqueous solutions of selected 1-alkyl sulfonates, namely sodium 1-octanesulfonate
 341 (K8S), sodium 1-decanesulfonate (K10S), and sodium 1-dodecanesulfonate (K12S).
 342 The present work establishes that co-ions like octanate and decanate (similarly to
 343 shorter acetate, propionate, and butyrate [25,48]) do not have any significant effect on
 344 the CMC and N_{agg} of SDS. In contrary, dodecanate ions show an influence on the
 345 micellization behavior of the surfactant. It seems that K12S molecules (of the same
 346 carbon chain length as SDS) may act as the surfactant's mimetics and be incorporated
 347 into its micelles. In other words, SDS does not recognize K12S molecules as the ones
 348 with a different structure and consequently allows them to participate in the
 349 formation of the surfactant's micelles. The presented results may have important
 350 implications to understand the nature of the interactions between surfactants and
 351 various electrolytes.

352 Acknowledgements

353 This research was supported by PL-Grid Infrastructure and TASK computational
354 center. We want to thank Dr. Łukasz Nierzwicki for his scientific advice.

355 References

- 356 [1] S. Ghosh, A. Ray, N. Pramanik, Self-assembly of surfactants: An overview on
357 general aspects of amphiphiles. *Biophysical Chemistry* **2020**, 265, 106429.
- 358 [2] E.J. Acosta, J.H. Harwell, D.A. Sabatini, Self-assembly in linker-modified
359 microemulsions. *Journal of Colloid and Interface Science* **2004**, 274, 652-664.
- 360 [3] J. Mata, D. Varade, P. Bahadur, Aggregation behavior of quaternary salt based
361 cationic surfactants. *Thermochimica Acta* **2005**, 428, 147-155.
- 362 [4] S. Chakraborty, A. Chakraborty, M. Ali, S.K. Saha, Surface and bulk properties of
363 dodecylbenzenesulphonate in aqueous medium: role of the nature of counterions.
364 *Journal of Dispersion Science and Technology* **2010**, 31, 209-215.
- 365 [5] P. Hansson, B. Jönsson, C. Ström, O. Söderman, Determination of micellar
366 aggregation numbers in dilute surfactant systems with the fluorescence quenching
367 method. *The Journal of Physical Chemistry B* **2000**, 104, 3496-3506.
- 368 [6] D. Khatua, A. Gupta, J. Dey, Characterization of micelle formation of
369 dodecylmethyl-N-2-phenoxyethylammonium bromide in aqueous solution. *Journal*
370 *of Colloid and Interface Science* **2006**, 298, 451-456.
- 371 [7] A. Patist, S.G. Oh, R. Leung, D.O. Shah, Kinetics of micellization: its significance
372 to technological processes. *Colloids and Surfaces A: Physicochemical and Engineering*
373 *Aspects* **2001**, 176, 3-16.
- 374 [8] P.J. Missel, N.A. Mazer, G.B. Benedek, C.Y. Young, M.C. Carey, Thermodynamic
375 analysis of the growth of sodium dodecyl sulfate micelles. *The Journal of Physical*
376 *Chemistry* **1980**, 84, 1044-1057.
- 377 [9] Y. Moroi, R. Humphry-Baker, M. Gratzel, Determination of micellar aggregation
378 number of alkylsulfonic acids by fluorescence quenching method. *Journal of Colloid*
379 *and Interface Science* **1987**, 119, 588-591.
- 380 [10] A. Chatterjee, S.P. Moulik, S.K. Sanyal, B.K. Mishra, P.M. Puri, Thermodynamics
381 of micelle formation of ionic surfactants: a critical assessment for sodium dodecyl
382 sulfate, cetyl pyridinium chloride and dioctyl sulfosuccinate (Na salt) by
383 microcalorimetric, conductometric, and tensiometric measurements. *The Journal of*
384 *Physical Chemistry B* **2001**, 105, 12823-12831.
- 385 [11] S.A. Buckingham, C.J. Garvey, G.G. Warr, Effect of head-group size on
386 micellization and phase behavior in quaternary ammonium surfactant systems. *The*
387 *Journal of Physical Chemistry* **1993**, 97, 10236-10244.
- 388 [12] Q. Xu, M. Nakajima, S. Ichikawa, N. Nakamura, P. Roy, H. Okadome, T. Shiina,
389 Effects of surfactant and electrolyte concentrations on bubble formation and
390 stabilization. *Journal of Colloid and Interface Science* **2009**, 332, 208-214.
- 391 [13] R.F. Tuddenham, A.E. Alexander, The effect of pressure on micelle formation in
392 soap solutions. *The Journal of Physical Chemistry* **1962**, 66, 1839-1842.

- 393 [14] A. Rahman, C.W. Brown, Effect of pH on the critical micelle concentration of
394 sodium dodecyl sulphate. *Journal of Applied Polymer Science* **1983**, *28*, 1331-1334.
- 395 [15] H. Kumar, J. Kaur, Influence of electrolyte and temperature on the aggregation
396 behaviour of mixed system consisting drug and anionic surfactant. *Journal of Physics:*
397 *Conference Series* **2020**, *1531*, 012102.
- 398 [16] P. Palladino, R. Ragone, Ionic strength effects on the critical micellar
399 concentration of ionic and nonionic surfactants: the binding model. *Langmuir* **2011**,
400 *27*, 14065-14070.
- 401 [17] D. Das, K. Ismail, Aggregation and adsorption properties of sodium dodecyl
402 sulfate in water–acetamide mixtures. *Journal of Colloid and Interface Science* **2008**, *327*,
403 198-203.
- 404 [18] H. Demissie, R. Duraisamy, Effects of electrolytes on the surface and micellar
405 characteristics of Sodium dodecyl sulphate surfactant solution. *Journal of Scientific and*
406 *Innovative Research* **2016**, *5*, 208-214.
- 407 [19] I.V. Rao, E. Ruckenstein, Micellization behavior in the presence of alcohols.
408 *Journal of Colloid and Interface Science* **1986**, *113*, 375-387.
- 409 [20] N. Scholz, T. Behnke, U. Resch-Genger, Determination of the critical micelle
410 concentration of neutral and ionic surfactants with fluorometry, conductometry, and
411 surface tension—a method comparison. *Journal of Fluorescence* **2018**, *28*, 465-476.
- 412 [21] A. Cornellas, L. Perez, F. Comelles, I. Ribosa, A. Manresa, M.T. Garcia, Self-
413 aggregation and antimicrobial activity of imidazolium and pyridinium based ionic
414 liquids in aqueous solution. *Journal of Colloid and Interface Science* **2011**, *355*, 164-171.
- 415 [22] A. Wołowicz, K. Staszak, Study of surface properties of aqueous solutions of
416 sodium dodecyl sulfate in the presence of hydrochloric acid and heavy metal ions.
417 *Journal of Molecular Liquids* **2020**, *299*, 112170.
- 418 [23] B. Naskar, A. Dey, S.P. Moulik, Counter-ion effect on micellization of ionic
419 surfactants: A comprehensive understanding with two representatives, sodium
420 dodecyl sulfate (SDS) and dodecyltrimethylammonium bromide (DTAB). *Journal of*
421 *Surfactants and Detergents* **2013**, *16*, 785-794.
- 422 [24] B.C. Paul, S.S. Islam, K. Ismail, Effect of acetate and propionate co-ions on the
423 micellization of sodium dodecyl sulfate in water. *The Journal of Physical Chemistry B*
424 **1998**, *102*, 7807-7812.
- 425 [25] I.M. Umlong, K. Ismail, Micellization behaviour of sodium dodecyl sulfate in
426 different electrolyte media. *Colloids and Surfaces A: Physicochemical and Engineering*
427 *Aspects* **2007**, *299*, 8-14.
- 428 [26] M.Z. Hasan, S. Mahbub, M.A. Hoque, M.A. Rub, D. Kumar, Investigation of
429 mixed micellization study of sodium dodecyl sulfate and
430 tetradecyltrimethylammonium bromide mixtures at different compositions: Effect of
431 electrolytes and temperatures. *Journal of Physical Organic Chemistry* **2020**, *33*, e4047.
- 432 [27] A. Tesmar, M.M. Kogut, K. Żamojć, O. Grabowska, K. Chmur, S.A. Samsonov, J.
433 Makowska, D. Wyrzykowski, L. Chmurzyński, Physicochemical nature of sodium
434 dodecyl sulfate interactions with bovine serum albumin revealed by interdisciplinary
435 approaches. *Journal of Molecular Liquids* **2021**, *340*, 117185.



- 436 [28] S. Jo, T. Kim, V.G. Iyer, W. Im, CHARMM-GUI: a web-based graphical user
437 interface for CHARMM. *Journal of Computational Chemistry* **2008**, *29*, 1859-1865.
- 438 [29] M.J. Abraham, T. Murtola, R. Schulz, S. Páll, J.C. Smith, B. Hess, E. Lindahl,
439 GROMACS: High performance molecular simulations through multi-level
440 parallelism from laptops to supercomputers. *SoftwareX* **2012**, *1*, 19-25.
- 441 [30] G.A. Tribello, M. Bonomi, D. Branduardi, C. Camilloni, G. Bussi, PLUMED 2:
442 New feathers for an old bird. *Computer Physics Communications* **2014**, *185*, 604-613.
- 443 [31] J. Huang, S. Rauscher, G. Nawrocki, T. Ran, M. Feig, B.L. De Groot, H.
444 Grubmüller, A.D. MacKerell, CHARMM36m: an improved force field for folded and
445 intrinsically disordered proteins. *Nature Methods* **2017**, *14*, 71-73.
- 446 [32] S. Nosé, A unified formulation of the constant temperature molecular dynamics
447 methods. *The Journal of Chemical Physics* **1984**, *81*, 511-519.
- 448 [33] M. Parrinello, A. Rahman, Polymorphic transitions in single crystals: A new
449 molecular dynamics method. *Journal of Applied Physics* **1981**, *52*, 7182-7190.
- 450 [34] T. Darden, D. York, L. Pedersen, Particle mesh Ewald: An $N \cdot \log(N)$ method for
451 Ewald sums in large systems. *The Journal of Chemical Physics* **1993**, *98*, 10089-10092.
- 452 [35] Y. Gao, J. Lee, I.P.S. Smith, H. Lee, S. Kim, Y. Qi, J.B. Klauda, G. Widmalm, S.
453 Khalid, W. Im, Charmm-gui supports hydrogen mass repartitioning and different
454 protonation states of phosphates in lipopolysaccharides. *Journal of Chemical*
455 *Information and Modeling* **2021**, *61*, 831-839.
- 456 [36] S. Jo, J.B. Lim, J.B. Klauda, W. Im, CHARMM-GUI Membrane Builder for mixed
457 bilayers and its application to yeast membranes. *Biophysical Journal* **2009**, *97*, 50-58.
- 458 [37] Y. Sugita, A. Kitao, Y. Okamoto, Multidimensional replica-exchange method for
459 free-energy calculations. *The Journal of Chemical Physics* **2000**, *113*, 6042-6051.
- 460 [38] S. Kumar, J.M. Rosenberg, D. Bouzida, R.H. Swendsen, P.A. Kollman, The
461 weighted histogram analysis method for free-energy calculations on biomolecules. I.
462 The method. *Journal of Computational Chemistry* **1992**, *13*, 1011-1021.
- 463 [39] L. Piñeiro, M. Novo, W. Al-Soufi, Fluorescence emission of pyrene in surfactant
464 solutions. *Advances in Colloid and Interface Science* **2015**, *215*, 1-12.
- 465 [40] M. Pal, R. Rai, A. Yadav, R. Khanna, G.A. Baker, S. Pandey, Self-aggregation of
466 sodium dodecyl sulfate within (choline chloride+ urea) deep eutectic solvent.
467 *Langmuir* **2014**, *30*, 13191-13198.
- 468 [41] M. Benrraou, B.L. Bales, R. Zana, Effect of the nature of the counterion on the
469 properties of anionic surfactants. 1. Cmc, ionization degree at the cmc and
470 aggregation number of micelles of sodium, cesium, tetramethylammonium,
471 tetraethylammonium, tetrapropylammonium, and tetrabutylammonium dodecyl
472 sulfates. *The Journal of Physical Chemistry B* **2003**, *107*, 13432-13440.
- 473 [42] F. Warsi, M.R. Islam, M.S. Alam, M. Ali, Exploring the effect of hydrophobic
474 ionic liquid on aggregation, micropolarity and microviscosity properties of aqueous
475 SDS solutions. *Journal of Molecular Liquids* **2020**, *310*, 113132.
- 476 [43] E. Fuguet, C. Ràfols, M. Rosés, E. Bosch, Critical micelle concentration of
477 surfactants in aqueous buffered and unbuffered systems. *Analytica Chimica Acta* **2005**,
478 *548*, 95-100.



- 479 [44] A.R. Tehrani-Bagha, J. Kärnbratt, J.E. Löfroth, K. Holmberg, Cationic ester-
480 containing gemini surfactants: Determination of aggregation numbers by time-
481 resolved fluorescence quenching. *Journal of Colloid and Interface Science* **2012**, 376, 126-
482 132.
- 483 [45] K. Maiti, D. Mitra, S. Guha, S.P. Moulik, Salt effect on self-aggregation of sodium
484 dodecylsulfate (SDS) and tetradecyltrimethylammonium bromide (TTAB):
485 Physicochemical correlation and assessment in the light of Hofmeister (lyotropic)
486 effect. *Journal of Molecular Liquids* **2009**, 146, 44-51.
- 487 [46] S. Hayashi, S. Ikeda, Micelle size and shape of sodium dodecyl sulfate in
488 concentrated sodium chloride solutions. *The Journal of Physical Chemistry* **1980**, 84,
489 744-751.
- 490 [47] S. Ikeda, S. Hayashi, T. Imae, Rodlike micelles of sodium dodecyl sulfate in
491 concentrated sodium halide solutions. *The Journal of Physical Chemistry* **1981**, 85, 106-
492 112.
- 493 [48] I.M. Umlong, K. Ismail, Micellization of AOT in aqueous sodium chloride,
494 sodium acetate, sodium propionate, and sodium butyrate media: a case of two
495 different concentration regions of counterion binding. *Journal of Colloid and Interface*
496 *Science* **2005**, 291, 529-536.
- 497 [49] S. Mahbub, M.R. Molla, M. Saha, I. Shahriar, M.A. Hoque, M.A. Halim, M.A.
498 Rub, M.A. Khan, N. Azum, Conductometric and molecular dynamics studies of the
499 aggregation behavior of sodium dodecyl sulfate (SDS) and cetyltrimethylammonium
500 bromide (CTAB) in aqueous and electrolytes solution. *Journal of Molecular Liquids*
501 **2019**, 283, 263-275.
- 502 [50] E. Dutkiewicz, A. Jakubowska, Effect of electrolytes on the physicochemical
503 behaviour of sodium dodecyl sulphate micelles. *Colloid and Polymer Science* **2002**, 280,
504 1009-1014.
- 505 [51] K. Glenn, A. van Bommel, S.C. Bhattacharya, R.M. Palepu, Self-aggregation of
506 binary mixtures of sodium dodecyl sulfate and polyoxyethylene alkyl ethers in
507 aqueous solution. *Colloid and Polymer Science* **2005**, 283, 845-853.
- 508 [52] N. Sultana, Role of ammonium ion on the aggregation and adsorption properties
509 of sodium dodecylsulfate. *Journal of Dispersion Science and Technology* **2018**, 39, 92-99.
- 510 [53] W. Humphrey, A. Dalke, K. Schulten, VMD: visual molecular dynamics. *Journal*
511 *of Molecular Graphics* **1996**, 14, 33-38.

